

Membrane protein regulators of melanoma pulmonary colonization identified using a CRISPRa screen and spontaneous metastasis assay in mice

Louise van der Weyden , Victoria Offord, Gemma Turner, Agnes Swiatkowska, Anneliese O. Speak, and David J. Adams*

Wellcome Sanger Institute, Cambridge CB10 1SA, UK

*Corresponding author: Experimental Cancer Genetics, Wellcome Sanger Institute, Wellcome Genome Campus, Hinxton, Cambridge CB10 1SA, UK.
Email: da1@sanger.ac.uk

Abstract

Metastasis is the spread of cancer cells to a secondary site within the body, and is the leading cause of death for cancer patients. The lung is a common site of metastasis for many cancer types, including melanoma. Identifying the genes involved in aiding metastasis of melanoma cells to the lungs is critical for the development of better treatments. As the accessibility of cell surface proteins makes them attractive therapeutic targets, we performed a CRISPR activation screen using a library of guide RNAs (gRNAs) targeting the transcription start sites of 2195 membrane protein-encoding genes, to identify genes whose upregulated expression aided pulmonary metastasis. Immunodeficient mice were subcutaneously injected in the flank with murine B16-F0 melanoma cells expressing dCas9 and the membrane protein library gRNAs, and their lungs collected after 14–21 days. Analysis was performed to identify the gRNAs that were enriched in the lungs relative to those present in the cells at the time of administration (day 0). We identified six genes whose increased expression promotes lung metastasis. These genes included several with well-characterized pro-metastatic roles (*Fut7*, *Mgat5*, and *Pcdh7*) that have not previously been linked to melanoma progression, genes linked to tumor progression but that have not previously been described as involved in metastasis (*Olf322* and *Olf441*), as well as novel genes (*Tmem116*). Thus, we have identified genes that, when upregulated in melanoma cells, can aid successful metastasis and colonization of the lung, and therefore may represent novel therapeutic targets to inhibit pulmonary metastasis.

Keywords: mouse; B16-F0; spontaneous metastasis; lung; melanoma; CRISPR activation; *Fut7*

Introduction

Metastasis is the spread of cells from the primary tumor, to a site elsewhere in the body, and is a major cause of morbidity and mortality in melanoma patients. It is a multi-step process in which the primary tumor cells must enter the bloodstream and/or lymphatics (intravasation), survive in the circulation, extravasate into the parenchyma of the target organ(s), and survive in the new environment. Survival and proliferation in this “foreign” microenvironment are necessary for the development of clinically apparent/relevant metastases; as the presence of circulating tumor cells is common in patients with a primary tumor but is not an accurate predictor of metastasis. In many cancers, including melanoma, clinically detectable metastases are primarily found only within a subset of organs, suggesting that interaction of the tumor cell with the specific microenvironment of the secondary tissue is critical. In patients with melanoma, metastasis to the lung is common and often the first clinically detectable site of visceral metastasis (reviewed in [Damsky et al. 2010](#)). Thus, controlling pulmonary metastasis is of critical importance for patients with melanoma.

Several of the key hallmarks of cancer involve altered expression of membrane proteins and the downstream signaling

pathways that they regulate. These have been widely used as biomarkers and therapeutic targets ([Lin et al. 2019](#)). Membrane proteins expressed on the cell surface represent particularly attractive drug/immunological targets due to their accessibility, such as the receptor tyrosine kinase AXL (which is frequently over-expressed in many cancer types) ([Boshuizen et al. 2018](#)) and the transmembrane calcium signal inducer TROP-2 (which is highly expressed in metastatic breast cancer) ([Rugo et al. 2020](#)). Indeed, with critical roles in mediating interactions between the tumor cells and their microenvironment, cell surface proteins are involved in key steps of the metastatic cascade, such as intravasation ([Conn et al. 2008](#)) and homing to the lung microvasculature ([Brown and Ruoslahti, 2004](#)).

CRISPR activation (CRISPRa) screens involve the use of a catalytically inactive version of Cas9 (“dCas9”) fused to transcriptional activator domains (such as VP64), and guide RNAs (gRNAs) that target the transcription start sites (TSSs) of genes. Binding of the dCas9 and gRNA to the TSS of a gene results in its transcriptional activation and thus increased expression of the encoded protein ([Horlbeck et al. 2016](#)). We previously applied CRISPRa technology to screen a membrane protein gRNA library for genes that enhanced melanoma cell colonization of the lung, in the

Received: March 06, 2021. Accepted: May 03, 2021

© The Author(s) 2021. Published by Oxford University Press on behalf of Genetics Society of America.

This is an Open Access article distributed under the terms of the Creative Commons Attribution License (<http://creativecommons.org/licenses/by/4.0/>), which permits unrestricted reuse, distribution, and reproduction in any medium, provided the original work is properly cited.

context of an “experimental metastasis assay” (van der Weyden *et al.* 2021). In the present study, we apply the same gRNA library in an alternative context, specifically the “spontaneous metastasis assay,” which examines the entire metastatic cascade, from growth of the cells in the primary tumor to their spread to a secondary site and eventual colonization of the organ. This screen identified membrane proteins whose upregulated expression in melanoma cells enhanced the ability of the cells to metastasize to the lung and survive and proliferate at that secondary site, and thus represent potential therapeutic targets and/or biomarkers.

Materials and methods

Mice

Immunodeficient NOD.CgPrkdc^{scid}, Il2rg^{tm1Wjl}/SzJ (NSGM) mice were originally obtained from JAX Laboratories and maintained as a core colony at the Sanger Institute Research Support Facility. The care and use of all mice in this study were in accordance with the Home Office guidelines of the UK and procedures were performed under a UK Home Office Project license (P6B8058B0), which was reviewed and approved by the Sanger Institute’s Animal Welfare and Ethical Review Body. All mice were housed in individually ventilated cages in a specific pathogen-free environment. Female NSGM mice aged 6–8 weeks were used in this study, with the diet, cage conditions, and room conditions of the mice as per previously reported (van der Weyden *et al.* 2017).

Cells

The B16-F0 mouse melanoma cell line was purchased from ATCC (CRL-6475), genetically validated (Del Castillo Velasco-Herrera *et al.* 2018), and maintained in DMEM with 10% (v/v) fetal calf serum (FCS) and 2 mM glutamine, 100 U/mL penicillin/streptomycin at 37°, 5% CO₂. The cell line was screened for the presence of mycoplasma and mouse pathogens (Charles River Laboratories, USA). B16-F0 cells stably expressing dCas9 (“dCas9-F0 cells”) were generated as described previously (van der Weyden *et al.* 2021).

CRISPR activation membrane protein screen

The mouse membrane protein (“m6”) mCRISPRa-v2 subpooled library generated by Jonathan Weissman (Horlbeck *et al.* 2016) consists of 10,975 gRNAs targeting the TSSs of 2195 genes that encode for membrane proteins, and 250 nontargeting control gRNAs, and was acquired from Addgene (#84003). The m6 library was re-amplified in liquid culture following Weismann lab protocols (<https://weissmanlab.ucsf.edu/CRISPR/CRISPR.html>) and the plasmid DNA extracted using an EndoFree Plasmid Mega Kit (Qiagen). The plasmid DNA was packaged into lentiviruses in HEK293T cells using LipofectamineTM LTX (ThermoFisher) and packaging plasmids pMD2.G (Addgene #12259) and psPAX2 (Addgene #12260). Sixteen hours after transfection, the medium was replaced with complete IMDM and ~30 hours later, the medium (containing the virus supernatant) was collected and filtered with a 0.45 μm low protein-binding filter (Merck). Transduction was carried out in dCas9-F0 cells at a multiplicity of infection (MOI) of 0.3 and 8 g/mL of polybrene and the medium was changed the following day. Three independent populations of dCas9-F0 cells were transduced and maintained separately (hereafter known as groups A, B, and C). After 48 hours, cells were passaged and 5 μg/mL of puromycin added to the medium. A sample of the transduced cells (and some untransduced cells as controls) were analyzed by flow cytometry (BD LSRFortessaTM) to measure the expression of blue fluorescent protein (BFP; a BFP cassette is present in the vector backbone of the “pCRISPRia_v2”

library plasmid) and confirm successful transduction. After a further 4 days, cells were passaged again and after 9 days, cells were detached, counted, centrifuged at 300 g for 5 minutes then diluted in phosphate-buffered saline (PBS). Two aliquots of 5.5×10^6 cells from each group (500x library representation) were pelleted and snap-frozen (representing “0-hour” timepoint) and aliquots of 5.5×10^5 cells from each group (50x library representation) in 100 μL PBS were subcutaneously administered into the right flank of 6–8 week old female NSGM mice. Groups A and B had 13 mice each, and group C had 14 mice (making a total of 40 mice). The primary tumor masses on the flank of the mice were measured using Vernier calipers every 1–3 days and the mice humanely sacrificed when the tumor reached ~2.5 cm² (width of the tumor × length of the tumor).

Processing the lung samples

The lungs from each mouse (all 5 lobes), as well as the “0-hour” timepoint dCas9-F0 cell pellets, were homogenized in 1 mL Tris-buffered saline with 0.5% Triton X-100 and a representative portion taken for genomic DNA (gDNA) extraction using the Purgene kit (Qiagen) according to manufacturer’s instructions. The gDNA (50 ug) was digested with SbfI HF (NEB) overnight (to enrich for gDNA containing the gRNA as SbfI sites flank the gRNA in the pCRISPRia_v2 vector) and the desired 471 bp product was purified using a Select-a-Size DNA Clean & Concentrator kit (Zymo) according to the manufacturer’s protocol. PCR reactions were performed with 500 ng of the 471 bp product per reaction, using the Phusion[®] High-Fidelity PCR Master Mix with HF Buffer (NEB) to amplify the gRNAs. The forward primer contained an 8mer barcode, 5’ Illumina adapters and homology to the CRISPRia-v2 plasmid and the reverse primer contained 3’ Illumina adapters and homology to the CRISPRia-v2 plasmid (Horlbeck *et al.* 2016). For each mouse/lung, 24 PCR reactions (of 35 cycles each) were performed and all products were pooled. PCR was also performed on duplicate 0-hour dCas9-F0 cell gDNA. Each set of pooled PCRs was purified using a Monarch[®] PCR & DNA Cleanup kit (NEB; to purify the 280 bp PCR product), followed by a Select-A-Size DNA Clean & Concentrator kit (Zymo; to remove the 150 bp primer-dimer), according to the manufacturer’s protocol. Purity and concentration of all PCR samples were confirmed by analysis on a Bioanalyser. The samples within each cohort of lungs and relevant “0-hour” timepoint samples (cohorts A–C) were pooled, and each cohort sequenced over 2 runs on a HiSeq2500 (Illumina). Two sequencing primers were used: a bespoke primer (GTG TGT TTT GAG ACT ATA AGT ATC CCT TGG AGA ACC ACC TTG TGG) and a standard Illumina primer.

Statistics and bioinformatic analysis

Single end 50 bp reads were trimmed to remove adapter sequences and compared for exact matches against the 11,225 sgRNAs (including 250 nontargeting controls) from the Weissman murine membrane proteins “m6” library (which only includes the “Top5” gRNAs) [<https://www.addgene.org/pooled-library/weissman-mouse-crispra-v2-subpools/>]. Guides with <30 reads in either of the “0-hour” timepoint replicates were removed from the resulting count matrix. To identify enriched gRNAs, the “percentile” method was used as previously described (van der Weyden *et al.* 2021). Briefly, total normalization was performed with MAGeCK (version 0.5.8) (Li *et al.* 2014), using the “0-hour” timepoint samples as the control, and gRNAs with no reads assigned were removed post-normalization. The samples from all 3 cohorts were pooled together for the analysis. For each gRNA, the following was determined: the number of samples (mice) in which it was

present (n), the count mean (m), standard deviation (SD), error of the mean (SEM ; calculated as SD divided by the square root of the group count), the z -score (determined as the normalized count minus the mean of the control counts, divided by the group SEM) and the number of samples (mice) in which it was present within the 98th percentile (n_{NEP} ; in terms of relative abundance of all gRNA reads in that mouse). gRNAs were ranked by the number of samples (mice) in which they were present in the 98th percentile, followed by z -score.

Data availability

The data underlying this article are available in the article and its online supplementary material. The CRISPRa data are available under the European Nucleotide Archive (ENA) accession number ERP127223.

Results

To identify membrane proteins whose increased expression enhances the ability of melanoma cells to metastasize to the lung, we performed a spontaneous metastasis assay in mice using the B16-F0 mouse melanoma cell line. In the spontaneous metastasis assay, tumor cells are orthotopically administered to the mouse and form a primary tumor mass over time; some of these cells may then metastasize (enter the circulation, travel to distant sites, and survive and proliferate at that secondary site). It has been shown previously that B16-F0 cells predominantly favor metastasizing to the lung (Deng et al. 2017), but they are weakly metastatic (Del Castillo Velasco-Herrera et al. 2018), thus, they were chosen to reduce the “background” of the screen (i.e., the number of cells that may metastasize to the lung regardless of the gRNA they are carrying). B16-F0 cells stably expressing dCas9 (F0-dCas9) were virally transduced with a CRISPRa gRNA library targeting genes that encode membrane proteins (Figure 1). The library contained 11,225 gRNAs in total, and was composed of gRNAs targeting 2195 membrane protein-encoding genes (with five gRNAs/gene) and 250 nontargeting “control” gRNAs, cloned into the pCRISPRia_v2 vector backbone (Horlbeck et al. 2016). Three populations of F0-dCas9 cells were virally transduced (experiments A, B, and C) and maintained separately throughout the experiment. Mice were subcutaneously administered with 5.5×10^5 cells from either experiment A, B, or C (representing a 50x coverage of the library).

Each experimental cohort was composed of 13–14 immunodeficient (“NSGM”) mice, with 40 mice in total. NSGM mice were used to avoid the issue of ulceration of the tumor mass which

occurred in a significant proportion of cases when we used immunocompetent mice (60%, $n = 36/60$ C57BL/6NTac mice, 60%). This can result in death of the mouse due to shock (even in tumors of $<1 \text{ cm}^2$) (Konger et al. 2017) and requires euthanasia as per Home Office-approved protocols. Ulceration of subcutaneously administered mouse melanoma B16 cells has been previously reported (van Elsas et al. 2001; Erkes et al. 2016; Konger et al. 2017), and ulceration of melanomas in humans carries a poor prognosis (Tas and Erturk 2021). The developing primary tumor in the flank of the NSGM mice was regularly measured and when it reached $\sim 2.5 \text{ cm}^2$ (average: $2.33 \pm 0.36 \text{ cm}^2$), which occurred 14–21 days post-dosing (average: 15.2 ± 2.1 days), the mice were humanely sacrificed and their lungs collected for analysis of pulmonary metastases. A “timepoint” of 2.5 cm^2 was set based on previous experience of the spontaneous metastasis model, as this allowed sufficient time for the cells in the developing mass to undergo pulmonary metastasis and colonize the lung, without allowing the subcutaneous mass to become too large (and risk impeding the locomotion of the mouse). Allowing the mass to continue growing, rather than surgical removal at a small size, avoids the issue of tumor cell seeding during surgery, which may contribute to metastasis formation by the tumor cells that enter the bloodstream (Pachmann 2011). All mice developed a primary tumor that reached the size limit set, however, at this timepoint, the metastases were only macroscopically visible in three of the mice. Details of the individual mice in each cohort, day sacrificed and presence of macroscopically visible lung metastases are shown in Supplementary Table S1.

Genomic DNA (gDNA) was extracted from the lungs of the mice in all 3 cohorts and high-throughput sequencing was performed to identify the gRNA representation in each mouse, relative to that present in the transduced B16-F0-dCas9 cell population before injection (i.e., “0-hour” timepoint). To identify gRNAs that were significantly enriched in the lungs of these mice, we used a “percentile ranking” (PR) approach (van der Weyden et al. 2021), to identify gRNAs found in the top 98th percentile of abundance/mouse (Figure 2). This method analyses each gRNA on an individual basis and does not consider the results of the four other gRNAs targeting TSSs of the same gene, as each TSS may not have an equal ability to regulate gene expression. When comparing the percentile ranking results across all 3 cohorts, the gRNAs were ranked by how often they appeared in the top 98th percentile, followed by their z -score (Supplementary Table S2). A biological filter was applied as we were only interested in determining robust (strong) regulators of metastasis and thus, we considered only those gRNAs found in

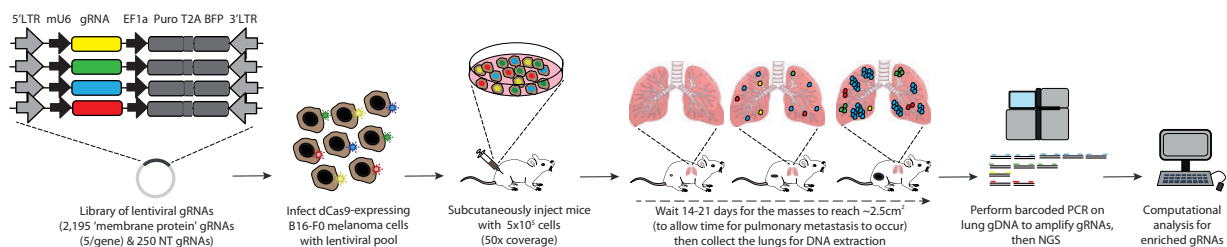


Figure 1 Schematic outline of the screen. dCas9-expressing B16-F10 mouse melanoma cells were transduced with a library of lentiviral gRNAs targeting the TSS of 2195 “membrane protein” genes (five gRNAs/gene) and 250 nontargeting (“NT”) controls. These cells (5.5×10^5 , which represents a 50-fold coverage of the library) were then subcutaneously injected into the flank of immunodeficient mice. The resulting masses were regularly measured and when they reached $\sim 2.5 \text{ cm}^2$ (sufficient time for metastasis and pulmonary colonization to have occurred; 14–21 days after administration of the tumor cells), the mice were humanely sacrificed. Their lungs were then collected for genomic DNA (gDNA) extraction and barcoded PCR was used to amplify the gRNAs present in the gDNA. The pooled PCRs were then sequenced using next-generation sequencing (NGS) and bioinformatic analysis was performed to identify the gRNAs that were enriched in each lung/mouse.

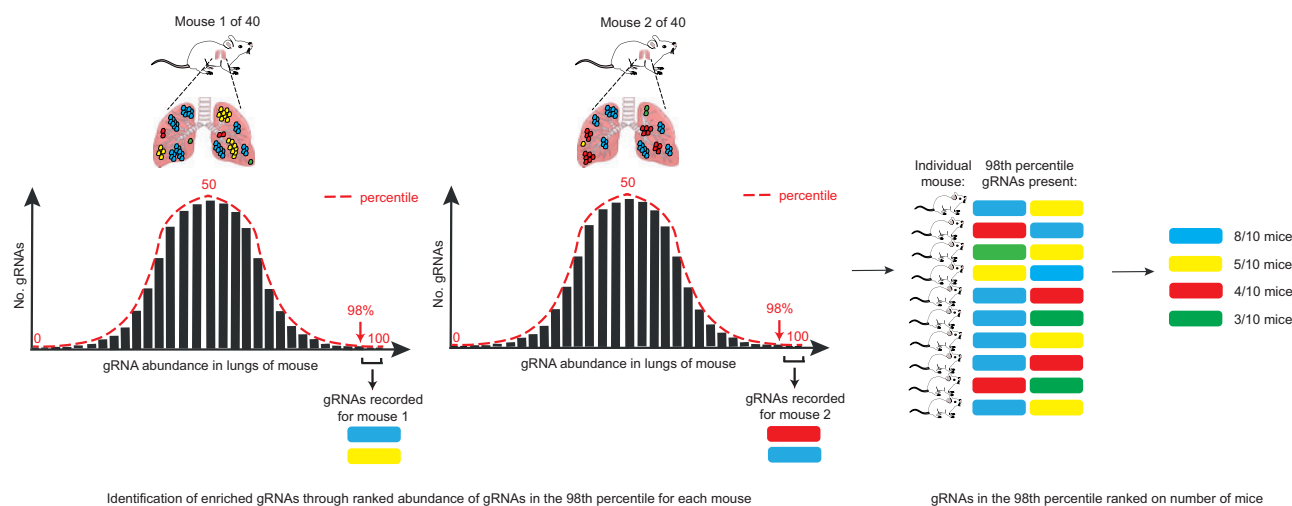


Figure 2 Schematic outline of the percentile ranking approach used to identify enriched gRNAs. To identify gRNAs that were significantly enriched in the lungs of the mice, the gRNAs found in the top 98th percentile of abundance in the lungs of each individual animal was determined. When comparing the percentile ranking results across all 3 cohorts (40 mice total), the gRNAs were then ranked by how often (*i.e.*, in how many mice) they were detected, followed by their z-score.

the 98th percentile in >30% of the mice. Using this filter, we classified six gRNAs as hit: *Fut7*, *Mgat5*, *Olf322*, *Olf441*, *Pcdh7*, and *Tmem116* (Table 1 and Supplementary Table S3). The gRNA that had abundance in the 98th percentile in the greatest number of mouse lungs (40%, 16/40) targeted a TSS of *Fut7*. The other five gRNAs had abundance in the 98th percentile in 32.5% of mice ($n = 13/40$).

Discussion

We previously performed an *in vivo* CRISPRa screen for membrane proteins whose upregulated expression resulted in enhanced metastatic colonization of the lung (van der Weyden *et al.* 2021). This was performed using an experimental metastasis assay in which mice were tail-vein dosed with dCas9-expressing B16-F0 cells transduced with a library of CRISPRa gRNAs targeting the TSS of membrane proteins. We identified several novel genes as playing a key role in pulmonary metastatic colonization, including *Lrm4cl*, *Slc4a3*, and *Tm4sf19*, and we performed an in-depth characterization of the mechanism of action of *Lrm4cl* (van der Weyden *et al.* 2021). In the current study, we used the same CRISPRa gRNA library, in the context of a different assay, to further interrogate the role of these membrane proteins in promoting metastasis. Specifically, we performed a “spontaneous metastasis assay,” whereby the tumor cells were subcutaneously

Table 1 Screen hits

Gene	No. mice	z-score
<i>Fut7</i>	16/40	10.76
<i>Olf441</i>	13/40	9.04
<i>Pcdh7</i>	13/40	8.73
<i>Mgat5</i>	13/40	8.54
<i>Tmem116</i>	13/40	8.47
<i>Olf322</i>	13/40	6.08

The gRNAs were ranked based on how many times they were found in the top 98th percentile of abundance (considered on a per-mouse basis). Hits were defined as those found in the 98th percentile of >30% of the mice ($n = 40$ mice in total). The number of mice in which the gRNAs were found in the 98th percentile and the z-score for the specific gRNA is shown. Details of the specific gRNAs and the mice in which they were identified are provided in Supplementary Tables S1 and S2.

administered to the mouse and the metastatic clones arising within the primary tumor spontaneously extravasate into the blood/lymphatic stream. In comparison to the experimental metastasis assay which administers the tumor cells directly into the bloodstream, the spontaneous metastasis assay also includes the early stages of the metastatic cascade, such as the growth of the primary tumor into the surrounding tissue, outgrowth of clones with metastatic potential, and invasion through the basement membrane and into the blood or lymphatic vessels (intravasation). This analysis implicated *Fut7*, *Mgat5*, *Pcdh7*, *Tmem116*, and olfactory receptors (ORs) *Olf441* and *Olf322* as drivers of pulmonary metastasis in melanoma cells, with gRNAs targeting the TSSs of these genes being found in the 98th percentile of relative abundance of gRNAs present in the lungs of $\geq 13/40$ mice. Although gRNAs targeting *Lrm4cl* were found in the 98th percentile in the lungs of 5/40 mice, they were not classified as a “hit” in this screen as we applied a biological filter of having to be found in the lungs of >30% of the mice. In addition, the differences between the assays are likely responsible for the differences in genes identified in the two studies. The experimental metastasis assay interrogates only the terminal stages of the very inefficient metastatic cascade, whereas the spontaneous metastatic assay includes the early steps that happen prior to arrest at the secondary site. Thus, whilst some degree of overlap might be expected in theory since the terminal stages of metastasis are captured in both assays, this requires each screen to have been performed to saturation. However, due to the complex and highly inefficient nature of metastasis, it is unlikely that this depth of analysis would have been achieved. Thus, it is not unexpected to have nonoverlapping gene sets given the numbers of mice ($n = 35\text{--}40$), cells (5.5×10^5), and gRNA fold coverage (only 50x) used in both screens.

For the genes implicated as drivers of melanoma pulmonary metastasis that were identified by the spontaneous metastasis assay, some have well-established roles in tumorigenesis and metastasis, whilst the function of others is relatively unknown.

Fut7

The *fucosyltransferase 7* (*Fut7*) gene encodes a Golgi alpha-(1,3)-fucosyltransferase enzyme that catalyzes the final fucosylation

step in the synthesis of the sialyl Lewis X antigen (sLe^x, also known as CD15s) (Sasaki et al. 1994). sLe^x can serve as a ligand for cell surface-expressed E-selectin or P-selectin and is involved in selectin-mediated adhesion of cancer cells to the vascular endothelium, a critical step in the metastatic process (Kannagi et al. 2004). Expression of FUT7 is related to poor prognosis in lung cancer (Ogawa et al. 1996) and sLe^x over-expression is associated with tumor metastasis, recurrence, and overall survival in patients with cancer (Liang et al. 2016). FUT7 expression is up-regulated at both mRNA and protein levels in hepatocellular carcinoma HepG2 cells, and an sLe^x-binding DNA aptamer effectively inhibited the interactions between E-selectin and sLe^x in HepG2 cells, resulting in reduced adhesion, migration, and invasion of the cells *in vitro* (Wang et al. 2017). *In vitro* studies in A549 lung cancer cell lines have shown that FUT7 overexpression augments sLe^x synthesis to trigger cell proliferation via the activation of the EGFR/AKT/mTOR signaling pathway (Liang et al. 2017). Lung cancer and glioma cell lines transfected with FUT7 cDNA showed increased expression of sLe^x and changed their characteristics from “nonmetastatic” to “metastatic”-like (including increased adhesion to a brain-derived endothelial cell monolayer and disruption of an *in vitro* blood-brain-barrier model) (Jassam et al. 2019). Thus, elevated FUT7 expression has a well-established role in metastasis and we show here for the first time that elevated Fut7 expression can promote the spontaneous metastasis of melanoma cells.

Mgat5

The *Mgat5* gene encodes the N-acetylglucosaminyltransferase-V enzyme (also known as GnT-V) that produces the β 1,6-linked N-acetylglucosamine (GlcNAc) branch on the α 1,6-mannose residue of N-glycans that are attached to cell surface or secreted glycoproteins (Gu et al. 1993). MGAT5 expression levels, which have been shown to be driven by the oncogenic RAS-RAF-ETS1 pathway (Kang et al. 1996; Buckhaults et al. 1997), are elevated in various cancer types (Zhao et al. 2008a, 2008b). Numerous studies have shown that β 1,6-branching of glycoproteins promotes tumor progression and metastasis. For example, the presence of β 1,6-branched oligosaccharides are increased in lymph node metastases and correlate with poor prognosis in breast carcinoma (Taeda et al. 1996) and increased β 1-6 branching in nonmetastatic murine mammary carcinoma cell clones strongly correlated with their acquisition of metastatic potential (Dennis et al. 1987). The β 1-6 branch modification allows target proteins to be covered with a number of N-acetylglucosamine (GlcNAc) residues, creating high-affinity ligands for galectins (Dennis et al. 2009) which can prolong the appearance of growth factor receptors on the cell surface (Boscher et al. 2011). The modification also regulates the adhesive properties of the cells by inhibiting cell adhesion and enhancing cell migration (Guo et al. 2009), thereby promoting tumor cell invasion and metastasis. Indeed, over-expression of MGAT5 in pre-malignant lung epithelial Mv1Lu cells resulted in reduced contact inhibition and adhesion, and increased cell motility and transformation (Demetriou et al. 1995). Tumor growth and metastasis are strongly suppressed in *Mgat5* knockout mice and cells (Granovsky et al. 2000; Guo et al. 2010).

Olfactory receptors

The olfactory receptor 322 (*Olf322*) and olfactory receptor 441 (*Olf441*) genes encode ORs which are members of a large family of G-protein coupled receptors involved in the sensory perception of smell. Whilst ORs are mainly distributed in olfactory neurons, they are also expressed in nonolfactory tissues, termed ectopic ORs. Ectopic ORs

have been reported to play an important role in tumor progression of many different cancer types (reviewed in Lee et al. 2019).

Olf322:

The human homolog of *Olf322* is olfactory receptor family 2 subfamily W member 3 (*OR2W3*); the proteins encoded by these genes share 85% amino acid identity. *OR2W3* is one of only 7 ORs whose expression was detected in the chronic myelogenous leukemia K562 cell line and white blood cells from patients with acute myeloid leukemia (Manteniotis et al. 2016). Over-expression of *OR2W3* has been postulated to play an important role in the development and progression pancreatic cancer, with elevated *OR2W3* expression detected in pancreatic cancer tissues by immunohistochemistry (relative to adjacent nontumorous tissue) and the expression of *OR2W3* correlating with clinical stage and lymph node metastasis (Shi et al. 2018). Similarly, a study investigating the abundance of all 408 human coding OR genes in 960 cases of invasive breast carcinoma and 56 human breast cancer cell lines found significant upregulation of *OR2W3* in a proportion of these tumors; particularly stage IV tumors and those significantly abundant in the expression of genes associated with breast tumor invasion (Masjedi et al. 2019). In addition, *OR2W3* upregulation was associated with reduced survival in invasive breast carcinoma, suggesting that it may be a potential breast cancer invasion marker, with possible roles in breast cancer progression and metastasis requiring further investigation (Masjedi et al. 2019). Our study would support a role for *OR2W3* in metastasis.

Olf441:

The human homolog of *Olf441* is olfactory receptor family A member 14 (*OR2A14*); the proteins encoded by these genes share 79–82% amino acid identity (depending on the transcript). A retroviral insertional mutagenesis screen for mediators of prostate cancer progression, found lung metastases with vector provirus tagging the *OR2A14* gene (3.5 kb downstream of the TSS) (Bii et al. 2018). In addition, OncoPrint™ analysis of gene expression between prostate patient tissue and unaffected tissue found *OR2A14* was significantly over-expressed ($P = 0.000145$) (Bii et al. 2018). Our study adds weight to the role of *OR2A14* in cancer progression.

Pcdh7

The *protocadherin-7* (*Pcdh-7*) gene encodes a transmembrane receptor that is a member of the cadherin superfamily. The protocadherin subset of the superfamily have well-established roles in cell adhesion and regulation of downstream signalling pathways (reviewed in Kahr et al. 2013). *PCDH7* expression is dysregulated in tumorigenesis, with both oncogenic and tumor-suppressive activities reported in a context-dependent manner. For example, decreased *PCDH7* expression has been reported in colorectal (Bujko et al. 2015), bladder (Lin et al. 2016), and gastric cancer (Chen et al. 2017). However, increased *PCDH7* expression has been reported in nonsmall cell lung cancer (Zhou et al. 2017) and castration-resistant prostate cancer/neuroendocrine prostate cancer (Shishodia et al. 2019). Increased *PCDH7* protein expression was observed during tumor progression in prostate cancer tissues and male TRAMP mice (which spontaneously develop prostate tumors following the onset of puberty) (Shishodia et al. 2019). Critically, *PCDH7* over-expression in breast and lung cancer cells has been shown to facilitate brain metastasis by promoting the assembly of carcinoma–astrocyte gap junctions composed of connexin 43 (Chen et al. 2016). Our findings would support a

role for PCHD7 over-expression in facilitating lung metastasis of melanoma.

Tmem116

The *transmembrane protein family member 116* (*Tmem116*) gene encodes a type 3a transmembrane protein with a predicted localization mainly in the endoplasmic reticulum (ER) (Wrzesiński et al. 2015). The transmembrane (TMEM) family brings together proteins of mostly unknown functions. Studies have shown that TMEM expression can be up- or down-regulated in tumor tissue relative to adjacent normal tissue and there is experimental evidence that TMEMs can function as oncogenes or tumor suppressor genes, with roles in tumor growth/progression, invasion, metastasis, and chemoresistance (though not all pathways have yet been identified) (reviewed in Schmit and Michiels, 2018). Little is known about the function of TMEM116, with only one study to date reporting a role in cancer; *TMEM116* expression was significantly down-regulated in clear cell renal carcinomas, which correlated with tumor grade, metastasis, and overall survival (Wrzesiński et al. 2015). Our findings would suggest the opposite for TMEM116 in melanoma, and as such it may be like TMEM97, which reportedly has decreased expression in some tumor types and increased expression in others (thus showing both tumor suppressive and oncogenic behaviors in a tissue-dependent context) (reviewed in Schmit and Michiels 2018).

Conclusions

In summary, we have used a spontaneous metastasis assay to screen a library of 2195 membrane protein-encoding genes to identify candidate positive regulators of metastasis in melanoma cell lines. Our screen identified 6 genes whose increased expression promotes the ability of melanoma cells to leave the primary tumor site in the skin, enter the circulation, travel to the lungs, extravasate into the lung parenchyma, and proliferate and successfully colonize the lung. Some of these genes have known roles in metastasis of a range of tumor types to a range of metastatic sites and others represent novel regulators of pulmonary metastasis. The novel candidates we identify will require further follow-up studies to understand their mechanistic contribution to melanoma metastasis, to validate their role in human disease, and to explore their potential as therapeutic targets.

Acknowledgments

The authors thank members of the CASM Support Lab (Wellcome Sanger Institute) for QC of the purified CRISPRa PCR products, the DNA Pipelines Operations (Wellcome Sanger Institute) for sequencing of the PCR products, and the Research Support Facility staff (Wellcome Sanger Institute) for the breeding and care of the mice used in this study.

Funding

This work was supported by grants from Cancer Research UK (C20510/A13031 to D.J.A.), the Wellcome Trust (WT098051 to D.J.A.), and ERC Combat Cancer (319661 to D.J.A.).

Conflicts of interest

None declared.

Literature cited

- Bii VM, Collins CP, Hocum JD, Trobridge GD. 2018. Replication-incompetent gammaretroviral and lentiviral vector-based insertional mutagenesis screens identify prostate cancer progression genes. *Oncotarget*. 9:15451–15463.
- Boscher C, Dennis JW, Nabi IR. 2011. Glycosylation, galectins and cellular signaling. *Curr Opin Cell Biol*. 23:383–392.
- Boshuizen J, Koopman LA, Krijgsman O, Shahrahi A, van den Heuvel EG, et al. 2018. Cooperative targeting of melanoma heterogeneity with an AXL antibody-drug conjugate and BRAF/MEK inhibitors. *Nat Med*. 24:203–212.
- Brown DM, Ruoslahti E. 2004. Metadherin, a cell surface protein in breast tumors that mediates lung metastasis. *Cancer Cell*. 5:365–374.
- Buckhaults P, Chen L, Fregien N, Pierce M. 1997. Transcriptional regulation of N-acetylglucosaminyltransferase V by the src oncogene. *J Biol Chem*. 272:19575–19581.
- Bujko M, Kober P, Mikula M, Ligaj M, Ostrowski J, et al. 2015. Expression changes of cell-cell adhesion-related genes in colorectal tumors. *Oncol Lett*. 9:2463–2470.
- Chen Q, Boire A, Jin X, Valiente M, Er EE, et al. 2016. Carcinoma-astrocyte gap junctions promote brain metastasis by cGAMP transfer. *Nature*. 533:493–498.
- Chen HF, Ma RR, He JY, Zhang H, Liu XL, et al. 2017. Protocadherin 7 inhibits cell migration and invasion through E-cadherin in gastric cancer. *Tumour Biol*. 101042831769755.39:1010428317697551.
- Conn EM, Madsen MA, Cravatt BF, Ruf W, Deryugina EI, et al. 2008. Cell surface proteomics identifies molecules functionally linked to tumor cell intravasation. *J Biol Chem*. 283:26518–26527.
- Damsky WE, Rosenbaum LE, Bosenberg M. 2010. Decoding melanoma metastasis. *Cancers (Basel)*. 3:126–163.
- Del Castillo Velasco-Herrera M, van der Weyden L, Nsengimana J, Speak AO, Sjöberg MK, et al. 2018. Comparative genomics reveals that loss of lunatic fringe (LFNG) promotes melanoma metastasis. *Mol Oncol*. 12:239–255.
- Demetriou M, Nabi IR, Coppolino M, Dedhar S, Dennis JW. 1995. Reduced contact-inhibition and substratum adhesion in epithelial cells expressing GlcNAc-transferase V. *J Cell Biol*. 130:383–392.
- Dennis JW, Laferte S, Waghorne C, Breitman ML, Kerbel RS. 1987. Beta 1-6 branching of Asn-linked oligosaccharides is directly associated with metastasis. *Science*. 236:582–585.
- Dennis JW, Nabi IR, Demetriou M. 2009. Metabolism, cell surface organization, and disease. *Cell*. 139:1229–1241.
- Deng W, McLaughlin SL, Klinke DJ. II, 2017. Quantifying spontaneous metastasis in a syngeneic mouse melanoma model using real time PCR. *Analyst*. 142:2945–2953.
- Erkes DA, Xu G, Daskalakis C, Zurbach KA, Wilski NA et al. 2016. Intratumoral infection with murine cytomegalovirus synergizes with PD-L1 blockade to clear melanoma lesions and induce long-term immunity. *Mol Ther*. 24:1444–1445.
- Granovsky M, Fata J, Pawling J, Muller WJ, Khokha R, et al. 2000. Suppression of tumor growth and metastasis in *Mgat5*-deficient mice. *Nat Med*. 6:306–312.
- Gu J, Nishikawa A, Tsuruoka N, Ohno M, Yamaguchi N, et al. 1993. Purification and characterization of UDP-N-acetylglucosamine: alpha-6-D-mannoside beta 1-6N-acetylglucosaminyltransferase (N-acetylglucosaminyltransferase V) from a human lung cancer cell line. *J Biochem*. 113:614–619.
- Guo HB, Johnson H, Randolph M, Pierce M. 2009. Regulation of homotypic cell-cell adhesion by branched N-glycosylation of N-cadherin extracellular EC2 and EC3 domains. *J Biol Chem*. 284:34986–34997.

- Guo HB, Johnson H, Randolph M, Nagy T, Blalock R, et al. 2010. Specific posttranslational modification regulates early events in mammary carcinoma formation. *Proc Natl Acad Sci USA*. 107:21116–21121.
- Horlbeck MA, Gilbert LA, Villalta JE, Adamson B, Pak RA, et al. 2016. Compact and highly active next-generation libraries for CRISPR-mediated gene repression and activation. *Elife*. 5:e19760.
- Jassam SA, Maheraly Z, Ashkan K, Pilkington GJ, Fillmore HL. 2019. Fucosyltransferase 4 and 7 mediates adhesion of non-small cell lung cancer cells to brain-derived endothelial cells and results in modification of the blood-brain-barrier: *in vitro* investigation of CD15 and CD15s in lung-to-brain metastasis. *J Neurooncol*. 143:405–415.
- Kahr I, Vandepoel K, van Roy F. 2013. Delta-protocadherins in health and disease. *Prog Mol Biol Transl Sci*. 116:169–192.
- Kang R, Saito H, Ihara Y, Miyoshi E, Koyama N, et al. 1996. Transcriptional regulation of the N-acetylglucosaminyltransferase V gene in human bile duct carcinoma cells (HuCC-T1) is mediated by Ets-1. *J Biol Chem*. 271:26706–26712.
- Kannagi R, Izawa M, Koike T, Miyazaki K, Kimura N. 2004. Carbohydrate-mediated cell adhesion in cancer metastasis and angiogenesis. *Cancer Sci*. 95:377–384.
- Konger RL, Derr-Yellin E, Travers JB, Ocana JA, Sahu RP. 2017. Epidermal PPAR γ influences subcutaneous tumor growth and acts through TNF- α to regulate contact hypersensitivity and the acute photoresponse. *Oncotarget*. 8:98184–98199.
- Lee SJ, Depoortere I, Hatt H. 2019. Therapeutic potential of ectopic olfactory and taste receptors. *Nat Rev Drug Discov*. 18:116–138.
- Li W, Xu H, Xiao T, Cong L, Love MI, et al. 2014. MAGeCK enables robust identification of essential genes from genome-scale CRISPR/Cas9 knockout screens. *Genome Biol*. 15:554.
- Liang JX, Liang Y, Gao W. 2016. Clinicopathological and prognostic significance of sialyl Lewis X overexpression in patients with cancer: a meta-analysis. *Oncol Targets Ther*. 9:3113–3125.
- Liang JX, Gao W, Cai L. 2017. Fucosyltransferase VII promotes proliferation via the EGFR/AKT/mTOR pathway in A549 cells. *Onco Targets Ther*. 10:3971–3978.
- Lin YL, Wang YL, Fu XL, Li WP, Wang YH, et al. 2016. Low expression of protocadherin7 (PCDH7) is a potential prognostic biomarker for primary non-muscle invasive bladder cancer. *Oncotarget*. 7:28384–28392.
- Lin CY, Lee CH, Chuang YH, Lee JY, Chiu YY, et al. 2019. Membrane protein-regulated networks across human cancers. *Nat Commun*. 10:3131.
- Mantoniotis S, Wojcik S, Brauhoff P, Möllmann M, Petersen L, et al. 2016. Functional characterization of the ectopically expressed olfactory receptor 2AT4 in human myelogenous leukemia. *Cell Death Discov*. 2:15070
- Masjedi S, Zwiebel LJ, Giorgio TD. 2019. Olfactory receptor gene abundance in invasive breast carcinoma. *Sci Rep*. 9:13736.
- Ogawa J, Inoue H, Koide S. 1996. Expression of alpha-1,3-fucosyltransferase type IV and VII genes is related to poor prognosis in lung cancer. *Cancer Res*. 56:325–329.
- Pachmann K. 2011. Tumor cell seeding during surgery-possible contribution to metastasis formations. *Cancers (Basel)*. 3:2540–2553.
- Rugo HS, Bardia A, Tolane SM, Arteaga C, Cortes J, et al. 2020. TROPiCS-02: A Phase III study investigating sacituzumab govitecan in the treatment of HR+/HER2- metastatic breast cancer. *Future Oncol*. 16:705–715.
- Sasaki K, Kurata K, Funayama K, Nagata M, Watanabe E et al. 1994. Expression cloning of a novel alpha 1,3-fucosyltransferase that is involved in biosynthesis of the sialyl Lewis x carbohydrate determinants in leukocytes. *J Biol Chem*. 269:14730–14737.
- Schmit K, Michiels C. 2018. TMEM Proteins in Cancer: a review. *Front Pharmacol*. 9:1345.
- Shi C-J, Zhao Y, Wang M, Tian R, Li X, et al. 2018. Clinical significance of expression of olfactory receptor family 2 subfamily W member 3 in human pancreatic cancer. *World Chinese J Digestol*. 26:1229–1233.
- Shishodia G, Koul S, Koul HK. 2019. Protocadherin 7 is overexpressed in castration resistant prostate cancer and promotes aberrant MEK and AKT signaling. *Prostate*. 79:1739–1751.
- Taeda Y, Nose M, Hiraizumi S, Ohuchi N. 1996. Expression of L-PHA-binding proteins in breast cancer: reconstitution and molecular characterization of β 1–6 branched oligosaccharides in three-dimensional cell culture. *Breast Cancer Res Tr*. 38:313–324.
- Tas F, Erturk K. 2021. Primary tumour ulceration in cutaneous melanoma: its role on TNM stages. *Jpn J Clin Oncol*. 51:192–198.
- van der Weyden L, Arends MJ, Campbell AD, Bald T, Wardle-Jones H, et al. 2017. Genome-wide *in vivo* screen identifies novel host regulators of metastatic colonization. *Nature*. 541:233–236.
- van der Weyden L, Harle V, Turner T, Offord V, Iyer V, et al. 2021. CRISPR activation screen in mice identifies novel membrane proteins enhancing pulmonary metastatic colonisation. *Comms Biol*. 4:395.
- van Elsas A, Suttmuller RP, Hurwitz AA, Ziskin J, Villasenor J, et al. 2001. Elucidating the autoimmune and antitumor effector mechanisms of a treatment based on cytotoxic T lymphocyte antigen-4 blockade in combination with a B16 melanoma vaccine: comparison of prophylaxis and therapy. *J Exp Med*. 194:481–489.
- Wang XK, Peng Y, Tao HR, Zhou FF, Zhang C, et al. 2017. Inhibition of adhesion and metastasis of HepG2 hepatocellular carcinoma cells *in vitro* by DNA aptamer against sialyl Lewis X. *J Huazhong Univ Sci Technol [Med Sci]*. 37:343–347.
- Wrzesiński T, Szlag M, Cieślowski WA, Ida A, Giles R, et al. 2015. Expression of pre-selected TMEMs with predicted ER localization as potential classifiers of ccRCC tumors. *BMC Cancer*. 15:518.
- Zhao Y, Sato Y, Isaji T, Fukuda T, Matsumoto A, et al. 2008a. Branched N-glycans regulate the biological functions of integrins and cadherins. *FEBS J*. 275:1939–1948.
- Zhao YY, Takahashi M, Gu JG, Miyoshi E, Matsumoto A, et al. 2008b. Functional roles of N-glycans in cell signaling and cell adhesion in cancer. *Cancer Sci*. 99:1304–1310.
- Zhou X, Updegraff BL, Guo Y, Peyton M, Girard L, et al. 2017. Protocadherin 7 acts through SET and PP2A to potentiate MAPK signaling by EGFR and KRAS during lung tumorigenesis. *Cancer Res*. 77:187–197.

Communicating editor: D. Threadgill